FEBS Letters

FEBS PRESS science publishing by scientists

Investigating the roles of T224 and T232 in the oxidation of cinnamaldehyde catalyzed by myxobacterial CYP260B1

Martin Litzenburger, Roberta Lo Izzo, Rita Bernhardt and Yogan Khatri*

Institut für Biochemie, Universität des Saarlandes, Saarbruecken, Germany

Correspondence
Y. Khatri, FR 8.3 Biochemistry, Saarland University, Building B2.2, 66123 Saarbruecken, Germany
Fax: +49 681 302 4739
Tel: +49 681 302 7762
E-mail: yogan.khatri@uni-saarland.de

***Present address**
University of Michigan, Life Sciences Institute, 210 Washtenaw Ave., Ann Arbor, MI 48109, USA

(Received 27 October 2016, revised 25 November 2016, accepted 1 December 2016, available online 24 December 2016)

doi:10.1002/1873-3468.12519

Edited by Miguel De la Rosa

Although the oxidation of aldehydes to carboxylic acids is mainly catalyzed by aldehyde dehydrogenases in nature, cytochromes P450 are also able to perform such reactions. In this study, we demonstrate the oxidation of cinnamaldehyde to cinnamic acid by the myxobacterial CYP260B1. Following our docking studies of the aldehyde, we generated T224A and T234A mutants of CYP260B1 by site-directed mutagenesis to disrupt the substrate positioning and proton delivery, respectively. Furthermore, we used the kinetic solvent isotope effect on the steady-state turnover of the substrate to investigate the reactive intermediate capable of performing the catalysis. Our results suggest that the aldehyde oxidation occurs via a nucleophilic attack of the ferric peroxoanion.

Keywords: aldehyde oxidation; CYP260B1; kinetic solvent isotope effect; *Sorangium cellulosum* So ce56

Cytochromes P450 (P450) are heme-thiolate containing monooxygenase enzymes found in all domains of life [1]. They catalyze a broad range of different reactions such as hydroxylation, epoxidation, dealkylation, or C–C cleavage [2–4]. P450s are also able to oxidize aldehydes to the corresponding acids [5].

There are several studies described for the oxidation of saturated, α,β-unsaturated, or α,β-branched aldehydes by P450s [5–10]. In addition, some studies also describe the decarbonylation and the formation of olefins for branched compounds such as cyclohexanecarboxaldehyde or methylated propionaldehydes [11,12]. The utilization of α,β-unsaturated aldehydes as substrates resulting predominantly into carboxylic acids was also shown for several P450s [5]. Interestingly, most of these studies were performed with xenobiotic metabolizing P450s such as CYP2B4, CYP1A2, or CYP2E9 [5,12]. In contrast, only little is known concerning aldehyde oxidation by microbial P450s. The most prominent example for a bacterial P450 capable of aldehyde oxidation is CYP102A1 ($P450_{BM3}$) and its oxidation of ω-oxo fatty acids to the corresponding dicarboxylic acids [8], whereby the reactive species has not been studied.

Two different reaction mechanisms are proposed to catalyze such an oxidation reaction, either by the hydrogen abstraction and rebound hydroxylation mechanism or by nucleophilic attack of the ferric peroxoanion [13] (see Scheme 1).

As shown in Scheme 1, pathway A is independent of protons, whereas pathway B is requiring protons for the product formation. To distinguish between these two pathways, the kinetic solvent isotope effect (KSIE) can be used [14,15]. Furthermore, the proton delivery inside the active site can also be disrupted by site-directed mutagenesis and replacing the

Abbreviations
AdR, Adrenodoxin reductase; Adx_{4-108}, Adrenodoxin (truncated form); KSIE, kinetic solvent isotope effect; P450, cytochrome P450; SOD, superoxide-dismutase.

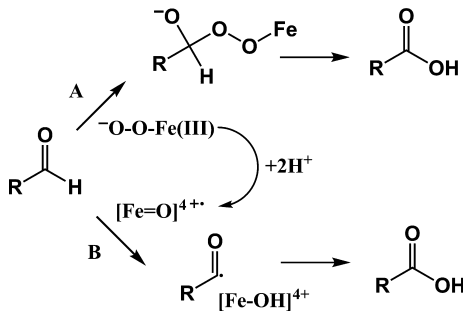

Scheme. 1. Proposed mechanisms for the oxidation of aldehydes to the corresponding acids. The nucleophilic attack by ferric peroxoanion (A), and the hydrogen abstraction and rebound reaction (B) are shown.

corresponding amino acids [16–18]. This approach was previously performed for mammalian CYP2B4 by creating the T302A variant to identify the reactive species capable of the conversion of aldehydes [6].

In this study, we demonstrate the oxidation of cinnamaldehyde to cinnamic acid by myxobacterial CYP260B1. In addition, docking of cinnamaldehyde into the crystal structure of CYP260B1 was performed followed by the creation of threonine mutants (T224A, T232A, and T224A/T232A). We investigated the KSIE for the oxidation reaction not only for the wild-type but also for the created threonine mutants T224A and T232A that are proposed to be involved in the substrate orientation and proton delivery, respectively.

Material and methods

Chemicals

Isopropyl β-D-1-thiogalactopyranoside and 5-aminolevulinic acid were purchased from Carbolution Chemicals (Saarbruecken, Germany). Bacterial media were obtained from Becton Dickinson (Heidelberg, Germany). All other chemicals were purchased from standard sources in the highest purity available.

Strains

The *Escherichia coli* strain top 10 for cloning purpose was obtained from Invitrogen (San Diego, USA). The *E. coli* strain C43(DE3) for the heterologous expression of the P450s was purchased from Novagen (Darmstadt, Germany).

Docking studies

The automated docking program AUTODOCK (version 4.20) [19,20] was applied for docking of cinnamaldehyde into the substrate-free crystal structure of CYP260B1 (PDB 5HIW) [21]. The Windows version 1.5.6 of AUTODOCK Tools was used to compute Kollman charges for the enzyme CYP260B1 and Gasteiger–Marsili charges for the ligands [22]. A partial charge of +0.400e was assigned manually to the heme-iron, which corresponds to Fe(II) that was compensated by adjusting the partial charges of the ligating nitrogen atoms to −0.348e. Flexible bonds of the ligands were assigned automatically and verified by manual inspection. A cubic grid box (56 × 56 × 56 points with a grid spacing of 0.375 Å) was centered 5 Å above the heme-iron. One hundred docking runs were carried out applying the Lamarckian genetic algorithm using default parameter settings.

Site-directed mutagenesis of CYP260B1

Targeted exchange of single amino acids was undertaken by QuikChange® mutagenesis with Pfu polymerase following manual instructions from Agilent Technologies (Santa Clara, USA). The corresponding forward and reversed primers for the T224A, T232A variants, and the T224A/T232A double mutant are shown in Table S1. The sequences of the mutants were verified by automated sequencing (Eurofins Genomics, Ebersberg, Germany).

Expression and purification of the enzymes

The expression and purification of CYP260B1 and its mutated variants were performed as described previously [21]. The truncated bovine adrenodoxin ($Adx_{4–108}$) and adrenodoxin reductase (AdR) were expressed and purified as described elsewhere [23,24].

Spectrophotometric characterization

UV–visible spectra for the purified P450s were recorded at room temperature with a double-beam spectrophotometer (UV-2101PC; Shimadzu, Kyoto, Japan). The proteins were diluted in 50 mM Tris/HCl buffer (pH 7.4) with 2% glycerol and the concentration of the P450s was estimated by CO difference spectroscopy assuming $\Delta\varepsilon$ (450–490) = 91 $mM^{-1} \cdot cm^{-1}$ according to the method of Omura and Sato [25]. Additionally, the P450s were measured in the reduced form as well as in the substrate-bound form. The proteins were reduced by the addition of a few grains of sodium dithionite and analyzed in the range of 300–700 nm. For the measurement of the substrate-bound form, the corresponding substrates were added in excess (2–5 times) and also analyzed in the range of 300–700 nm.

In vitro conversions and steady-state kinetic turnover

A reconstituted *in vitro* system containing the corresponding CYP260B1 variant (0.3 μM), AdR (0.9 μM), and $Adx_{4–108}$ (6 μM) in a final volume of 500 μL of Tris buffer

(50 mM, pH 7.4) with 2% glycerol was used. Cinnamaldehyde (dissolved in EtOH) was added to a final concentration of 100 μM. The reaction was started by the addition of NADPH (250 μM). After 30 min at 30 °C, the reaction was quenched by adding 10 μL HCl (1 : 1 diluted with water). The aqueous phase was extracted twice with chloroform (2 × 500 μL). A negative control in the absence of P450 in the reaction sample was employed for each substrate to verify the P450-dependent reaction. Likewise, the conversion of progesterone (200 μM final concentration) was performed except that samples were extracted immediately without acidification.

The steady-state kinetic turnover measurements of cinnamaldehyde were performed in protiated and deuterated solvent systems. To investigate the effect of radical scavengers on the catalytic rate, the *in vitro* conversions were performed with the addition of ascorbate (20 mM), catalase (20 U), and superoxide-dismutase (SOD, 3 U), individually as well as in combination.

HPLC analyses

HPLC analyses were performed on a system consisting of a PU-2080 HPLC pump, an AS-2059-SF autosampler, and a MD-2010 multi wavelength detector (Jasco; Gross-Umstadt, Germany). A Nucleodur 100–5 C18 column (125 × 4 mM; Macherey–Nagel, Düren, Germany) was used at 40 °C. Water with 0.1% trifluoroacetic acid (A) and acetonitrile with 0.1% trifluoroacetic acid (B) were used as mobile phases. A gradient from 25% to 55% B over 10 min was used for separation. For quantification of the compounds, calibration curves in the range of 0–200 μM were used. HPLC analyses of progesterone were performed with 10% acetonitrile in water (A) and acetonitrile (B) as mobile phases. A gradient of 10–60% B over 30 min was used for separation of the analytes.

Whole-cell conversions

The whole-cell conversion was performed according to the method previously described [26]. Cinnamaldehyde (200 μM) conversion was performed in eight sealed baffled flasks (1 L) each filled with 200 mL of M9CA medium. After 48 h, the reaction was quenched and extracted two times with the same volume of ethyl acetate. The crude extract was evaporated to dryness and stored at 4 °C until purification.

Purification of the product

The extract of the cinnamaldehyde conversion was purified by silica gel chromatography (hexane: ethyl acetate – 7 : 3). Fractions were collected and analyzed by thin layer chromatography. An UV lamp at 254 nm was used for the detection of the desired product. Product containing fractions were pooled and the solvent was removed by vacuum evaporation. About 23 mg of a light yellowish solid was obtained.

NMR analysis

NMR spectra were recorded on a Bruker (Rheinstetten, Germany) DRX 500 NMR spectrometer. A combination of ^{1}H, ^{13}C, and HSQC experiments was used for structure elucidation. All chemical shifts are relative to $CHCl_3$ (δ = 7.24 for ^{1}H NMR) or $CDCl_3$ (δ = 77.00 for ^{13}C NMR) using the standard δ notion in parts per million (p.p.m.).

trans-Cinnamic acid: ^{1}H NMR ($CDCl_3$, 500 MHz): 7.62 (d, 1H, J = 16.0 Hz, vinylic C–H), 7.38 (m, 2H, aromatic C–H), 7.23 (m, 3H, aromatic C–H), 6.29 (d, 1H, J = 16.0 Hz, vinylic C–H); ^{13}C NMR ($CDCl_3$, 125 MHz): 172.1 (C=O), 147.0 (C–H), 134.0 (C), 130.7 (C–H), 128.9 (C–H, 2x), 128.3 (C–H, 2x), 117.3 (C–H).

Results

Substrate identification and product elucidation

As CYP260B1 from *Sorangium cellulosum* So ce56 is known for the conversion of small compounds such as ionones and damascones [27], we tested cinnamaldehyde, a molecule of similar size containing an α,β-unsaturated aldehyde group. This compound served as a substrate and the conversion showed a single product (see Fig. 1). With our previously established whole-cell system [26], we were able to produce a sufficient amount of product for NMR analysis. The obtained product was identified as cinnamic acid.

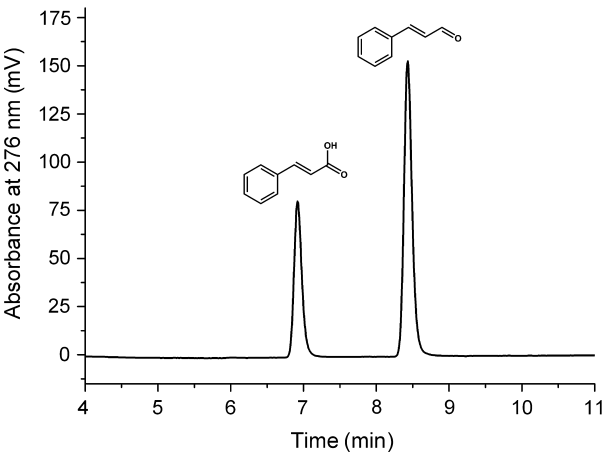

Fig. 1. The chromatogram shows the conversion of cinnamaldehyde (t_R = 8.4 min) to cinnamic acid (t_R = 6.9 min) catalyzed by CYP260B1.

Site-directed mutagenesis

Very recently, we have elucidated the crystal structure of CYP260B1 [21]. In order to get a deeper insight into the active site of this enzyme and the substrate orientation, we performed docking studies of cinnamaldehyde into the substrate-free crystal structure of CYP260B1 (see Fig. 2). The docking study showed that threonine 224 is suggested for the positioning of cinnamaldehyde. In addition, the amino acid sequence alignment of CYP260B1 with other P450s showed that threonine 232 is the conserved residue found in most P450s and is located in the I-helix next to a glutamic acid. This acid–alcohol pair is supposed to be involved in the proton delivery and catalysis [28]. The involvement of the conserved threonine in proton delivery was previously exemplified for the mutant T252A of CYP101A1 (P450cam) [29] or T306A of CYP17A1 [16].

To study the effect of T224 and T232, both amino acids were individually replaced by alanine resulting into the T224A and T232A variants. In addition, a double mutant in which both threonines were replaced by alanine (T224A/T232A) was also created.

Characterization of the mutants by UV–Vis spectroscopy and SDS/PAGE

The purified protein mutants were analyzed by SDS/PAGE and showed a molecular mass of about 50 kDa (see Fig. S1). Furthermore, the enzymes were characterized by UV–Vis spectroscopy (see Table S2 and Fig. S2).

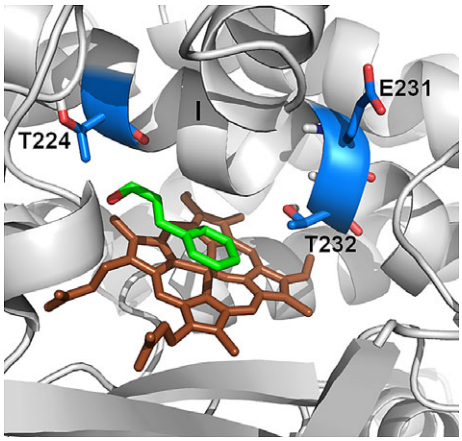

Fig. 2. Docking of cinnamaldehyde (green) into the substrate-free crystal structure of CYP260B1. The I-helix highlighting T224, E231, and T232 (blue cartoon) above the heme-plane (brown) is shown.

Functional characterization of the mutants by conversions of cinnamaldehyde and progesterone

To identify the functional properties of the novel CYP260B1 variants, conversions were performed with cinnamaldehyde as well as the known substrate progesterone [21]. This steroid was chosen for the functional characterization, as this compound was converted more efficiently by CYP260B1 compared with carotenoid-derived aroma compounds.

As shown in Table 1, all variants were able to convert both substrates; however, the product yields differed strongly. The conversion of cinnamaldehyde was decreased to almost half of the activity of the wild-type by the T224A variant. The predicted substrate orientation indicated that the phenyl ring is placed toward the heme-plane, which is not in accordance with the formed product. Nevertheless, this amino acid influenced the productivity toward cinnamic acid demonstrating its function in product formation. CYP260B1 and the T224A mutant converted the same amounts of progesterone but the product pattern was shifted toward a higher selectivity for T224A (see Fig. S3), which is in agreement with our assumption that this amino acid is important for substrate orientation.

The conversion of cinnamaldehyde was only slightly decreased by the T232A mutant. In contrast, the activity of this mutant toward the conversion of progesterone was significantly impaired (~ 10%) compared with the activity of the wild-type. This observation suggests that the steroid conversion is dependent on the presence of protons, whereas the oxidation of cinnamaldehyde seems to be independent on the presence of protons.

The double mutant (T224A/T232A) reflected the effects of the single mutants, in which the progesterone conversion was as strongly inhibited as shown for the T232A mutant. For the cinnamaldehyde conversion, the double mutant showed a similar effect as the T224A mutant; however, its activity was still higher

Table 1. Conversions of cinnamaldehyde and progesterone by CYP260B1, T224A mutant, T232A mutant, and T224A/T232A double mutant.

	Relative conversion by (%)			
Substrate	CYP260B1 (control)	T224A mutant	T232A mutant	T224A/T232A double mutant
Cinnamaldehyde	100	52	84	64
Progesterone	100	100	9	12

than that of the T224A variant and might be explained by some conformational changes inside the active site caused by replacing two threonines with the smaller amino acid alanine. The spectrum of the double mutant in cinnamaldehyde-bound form showed a shoulder at 393 nm (see Table S2 and Fig. S2) representing a small type-I shift induced by this substrate indicating a conformational change.

Steady-state turnover of cinnamaldehyde in protiated and deuterated solvent systems

As the conversions with the mutants indicated that cinnamaldehyde oxidation is independent of protons, the reactions were performed in both water and deuterium oxide to determine the KSIE (k_H/k_D) at steady state (see Fig. 3A,B). The activity in deuterated solvent was slightly higher than the reaction in protiated solvent with an inverse KSIE of about 0.9.

The catalytic cycle of P450s contains three unproductive pathways, in which the electrons are funneled for the production of superoxides (auto-oxidation shunt), hydrogen peroxide (peroxide shunt), or water (oxidase shunt), respectively [28]. To investigate the potential role of a H_2O_2-mediated conversion as well as the influence of unproductive pathways, diverse radical scavengers such as ascorbate (neutralizing the superoxide radical, singlet oxygen, and hydroxyl radicals), catalase (decomposing hydrogen peroxide to water and oxygen), and SOD (scavenger of superoxide anion) were applied individually as well as in combination. However, none of the scavengers showed a considerable effect on the conversion rate (see Fig. 3C). Additionally, the reactions were performed in the presence of H_2O_2, as the oxidation of cinnamldehyde can be mediated by H_2O_2 in the presence of transition metals [30]. As shown in Fig. 3C, H_2O_2 was able to produce low amounts of cinnamic acid, though its yield can be neglected compared to the control. All these results suggest that the reaction is catalyzed by a nucleophilic attack of the ferric peroxoanion and not mediated by a hydrogen abstraction and rebound mechanism.

The effect of the KSIE was also tested for the created mutants (see Fig. 4). Both the single mutants and the double mutant were not considerably influenced by the radical scavengers (see Fig. S4). In addition, all variants showed a higher conversion rate for the deuterated solvent system compared with the protiated one resulting in an inverse KSIE of 0.6 and 0.9 for T224A and T232A, respectively, and a KSIE of about 0.9 for the double mutant. The T232A variant showed a conversion rate of ~ 2 nmol product per minute per nmol P450 which is similar to the conversion rate of the wild-type suggesting that a disrupted proton delivery is not influencing the activity. We observed that neither the application of the deuterated solvent system nor employing the T232A variant or the combination of both approaches showed a considerably decreased cinnamic acid formation. This observation corroborated with the assumption of a nucleophilic attack by the ferric peroxoanion as most probable reaction mechanism for the aldehyde conversion.

Discussion

In plants, cinnamic acid is an important intermediate in the phenylpropanoid pathway that is further hydroxylated in position 4 by P450s (also known as cinnamate 4-hydroxylases) [31] resulting in *p*-coumaric acid, a precursor for the biosynthesis of several secondary metabolites such as lignins, coumarins, or

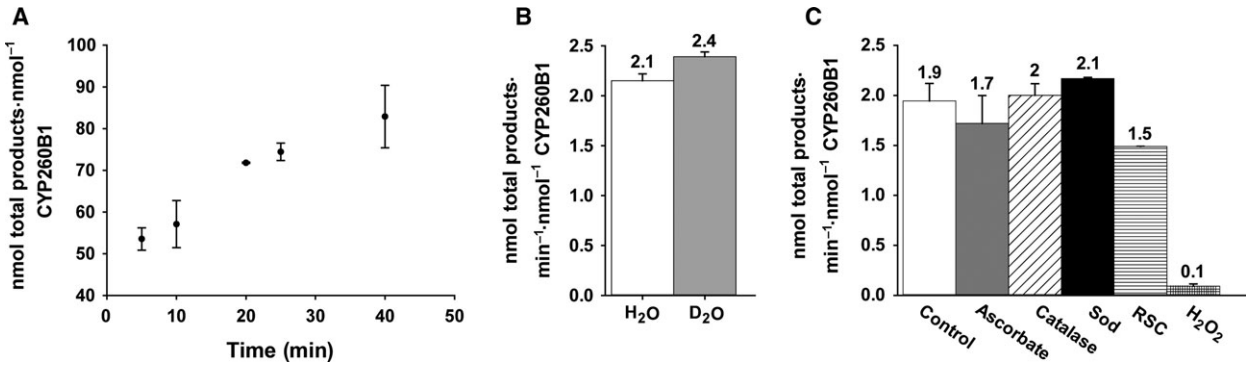

Fig. 3. Time-dependent conversion of cinnamaldehyde by CYP260B1 (A). The rate of conversion of the substrate in protiated and deuterated solvent systems (B), and the effect of radical scavengers (C) are shown. RSC, radical scavengers in combination. Results are obtained from triplicate experiments ± standard deviation.

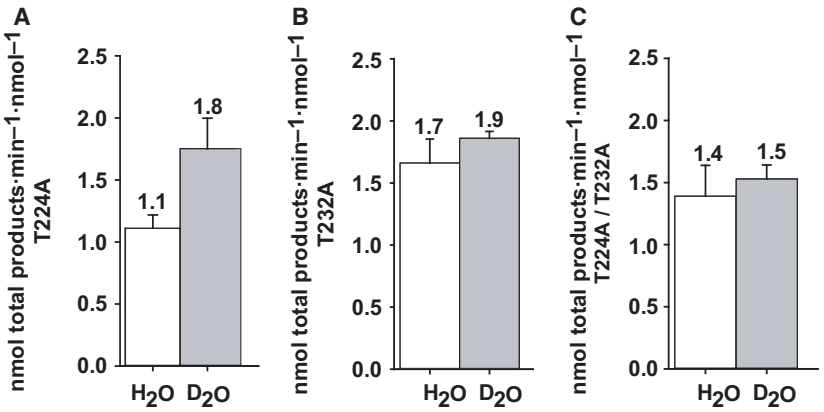

Fig. 4. The conversion rates of T224A (A), T232A (B), and double mutant (C) in protiated and deuterated solvent systems.

flavonoids [32]. Thereby, cinnamic acid is produced by deamination of the amino acid phenylalanine [33]. In this study, we demonstrated the formation of cinnamic acid by oxidation of cinnamaldehyde, an important compound for the flavor and fragrance industry [34], catalyzed by myxobacterial CYP260B1. This enzyme belongs to a novel P450 family found in *S. cellulosum* So ce56 [35] and is known for the conversion of steroids and carotenoid-derived aroma compounds [21,27]. It is not surprising that besides carotenoid-derived aroma compounds, cinnamaldehyde acts as substrate, as they are similar in size and functional groups. Interestingly, this substrate was not functionalized in an endocyclic position as demonstrated for some carotenoid-derived aroma compounds. Reasons for that observation might be related to the substrate orientation caused by the structural differences such as the phenyl ring or by the presence of the highly reactive α, β-unsaturated aldehyde moiety.

As the oxidation of aldehydes is supposed to be catalyzed by either ferryl species or ferric peroxoanion [13], we performed studies such as KSIE and site-directed mutagenesis to get a deeper insight into the reactive species capable of aldehyde oxidation. The activity was thereby neither considerably decreased by employing a deuterated solvent system nor by the T232A variant disrupting the proton transfer. Thus, both approaches supported the assumption of a proton-independent reaction catalyzed by nucleophilic attack of the ferric peroxoanion and not by hydrogen abstraction and rebound reaction. The functionality of the T232A variant was also tested by the progesterone conversion, which, however, showed only about 10% of the activity compared with the wild-type. The most common reaction for steroid functionalization is the hydroxylation, which is performed by the proton-dependent ferryl species [36]. With a disrupted proton delivery to the active site, this kind of reaction should be drastically decreased as shown here. As a result, the functionality of this amino acid can be confirmed. Concerning the function of T224, our docking studies suggested that this position is important for substrate positioning. This assumption was verified by the altered product pattern of the progesterone conversion (see Fig. S3). The wild-type showed a higher selectivity toward product number 5, whereas T224A favored the formation of product 3. In contrast, the product pattern of cinnamaldehyde conversion was not changed, although the activity was strongly influenced proving the influence of this amino acid toward the productivity. However, the predicted docking position cannot explain why the side chain is oxidized, as the phenyl group seems to be centered above the heme-plane. For that reason, another substrate orientation might be more probable for substrate oxidation or the substrate may be more mobile than indicated by the docking study.

Several studies on various mammalian P450s have described the oxidation of structural diverse aldehydes to their corresponding acids [5–7,9,37], among which CYP2B4 is the best-studied P450, and it was shown that the acid production is mainly catalyzed by the ferryl species by this enzyme [6]. In contrast, the peroxoanion-dependent reaction led to several other products such as alcohols or olefins. Some of the formed intermediates were also able to interact with the P450 itself leading to an inactivation of the enzyme [6,38]. However, such an adduct-based inactivation was predominantly found at higher substrate concentrations of several hundred micromolars. During the conversion of cinnamaldehyde by CYP260B1, neither side products nor a significant loss in its activity were observed, which might be related with a specific conformation of the active site hindering a deformylation

reaction. In addition, only low substrate concentrations were used for the CYP260B1-dependent reaction.

In conclusion, these results show the oxidation of cinamaldehyde to cinnamic acid by myxobacterial CYP260B1. Moreover, our results suggested that the ferric peroxoanion species is capable of catalyzing this type of reaction instead of the often proposed ferryl species.

Acknowledgements

The authors thank Birgit Heider-Lips for the purification of AdR and Adx and Dr. Josef Zapp for measuring the NMR sample. This work is supported by a grant of the Deutsche Forschungsgemeinschaft (Be1343/23-2) to RB.

Author contributions

ML, RB, and YK designed the project. ML, RLI, and YK carried out the experiments and analyzed the data. ML wrote the manuscript together with contributions from RB and YK. All authors read and approved the manuscript.

References:

1 Nelson DR (2011) Progress in tracing the evolutionary paths of cytochrome P450. *Biochim Biophys Acta* **1**, 14–18.

2 Sono M, Roach MP, Coulter ED and Dawson JH (1996) Heme-containing oxygenases. *Chem Rev* **96**, 2841–2888.

3 Bernhardt R (2006) Cytochromes P450 as versatile biocatalysts. *J Biotechnol* **124**, 128–145.

4 Bernhardt R and Urlacher VB (2014) Cytochromes P450 as promising catalysts for biotechnological application: chances and limitations. *Appl Microbiol Biotechnol* **98**, 6185–6203.

5 Amunom I, Stephens LJ, Tamasi V, Cai J, Pierce WM Jr, Conklin DJ, Bhatnagar A, Srivastava S, Martin MV, Guengerich FP *et al.* (2007) Cytochromes P450 catalyze oxidation of alpha, beta-unsaturated aldehydes. *Arch Biochem Biophys* **464**, 187–196.

6 Raner GM, Chiang EW, Vaz AD and Coon MJ (1997) Mechanism-based inactivation of cytochrome P450 2B4 by aldehydes: relationship to aldehyde deformylation via a peroxyhemiacetal intermediate. *Biochemistry* **36**, 4895–4902.

7 Raner GM, Vaz AD and Coon MJ (1996) Metabolism of all-trans, 9-cis, and 13-cis isomers of retinal by purified isozymes of microsomal cytochrome P450 and mechanism-based inhibition of retinoid oxidation by citral. *Mol Pharmacol* **49**, 515–522.

8 Davis SC, Sui Z, Peterson JA and Ortiz de Montellano PR (1996) Oxidation of omega-oxo fatty acids by cytochrome P450BM-3 (CYP102). *Arch Biochem Biophys* **328**, 35–42.

9 Bell-Parikh LC and Guengerich FP (1999) Kinetics of cytochrome P450 2E1-catalyzed oxidation of ethanol to acetic acid via acetaldehyde. *J Biol Chem* **274**, 23833–23840.

10 Sivaramakrishnan S, Ouellet H, Matsumura H, Guan S, Moenne-Loccoz P, Burlingame AL and Ortiz de Montellano PR (2012) Proximal ligand electron donation and reactivity of the cytochrome P450 ferric-peroxo anion. *J Am Chem Soc* **134**, 6673–6684.

11 Vaz ADN, Roberts EA and Coon MJ (1991) Olefin formation in the oxidative deformylation of aldehydes by cytochrome P-450. Mechanistic implications for catalysis by oxygen-derived peroxide. *J Am Chem Soc* **113**, 5886–5887.

12 Roberts ES, Vaz AD and Coon MJ (1991) Catalysis by cytochrome P-450 of an oxidative reaction in xenobiotic aldehyde metabolism: deformylation with olefin formation. *Proc Natl Acad Sci U S A* **88**, 8963–8966.

13 Guengerich FP, Sohl CD and Chowdhury G (2011) Multi-step oxidations catalyzed by cytochrome P450 enzymes: processive vs. distributive kinetics and the issue of carbonyl oxidation in chemical mechanisms. *Arch Biochem Biophys* **507**, 126–134.

14 Kiss FM, Khatri Y, Zapp J and Bernhardt R (2015) Identification of new substrates for the CYP106A1-mediated 11-oxidation and investigation of the reaction mechanism. *FEBS Lett* **589**, 2320–2326.

15 Gregory MC, Denisov IG, Grinkova YV, Khatri Y and Sligar SG (2013) Kinetic solvent isotope effect in human P450 CYP17A1-mediated androgen formation: evidence for a reactive peroxoanion intermediate. *J Am Chem Soc* **135**, 16245–16247.

16 Khatri Y, Gregory MC, Grinkova YV, Denisov IG and Sligar SG (2014) Active site proton delivery and the lyase activity of human CYP17A1. *Biochem Biophys Res Commun* **443**, 179–184.

17 Raag R, Martinis SA, Sligar SG and Poulos TL (1991) Crystal structure of the cytochrome P-450CAM active site mutant Thr252Ala. *Biochemistry* **30**, 11420–11429.

18 Vidakovic M, Sligar SG, Li H and Poulos TL (1998) Understanding the role of the essential Asp251 in cytochrome p450cam using site-directed mutagenesis, crystallography, and kinetic solvent isotope effect. *Biochemistry* **37**, 9211–9219.

19 Huey R, Morris GM, Olson AJ and Goodsell DS (2007) A semiempirical free energy force field with charge-based desolvation. *J Comput Chem* **28**, 1145–1152.

20 Morris GM, Goodsell DS, Halliday RS, Huey R, Hart WE, Belew RK and Olson AJ (1998) Automated docking using a Lamarckian genetic algorithm and an

empirical binding free energy function. *J Comput Chem* **19**, 1639–1662.
21 Salamanca-Pinzon SG, Khatri Y, Carius Y, Keller L, Muller R, Lancaster CR and Bernhardt R (2016) Structure-function analysis for the hydroxylation of Delta4 C21-steroids by the myxobacterial CYP260B1. *FEBS Lett* **590**, 1838–1851. doi:10.1002/1873-3468.12217. Epub 2016 Jun 3.
22 Sanner MF (1999) Python: a programming language for software integration and development. *J Mol Graph Model* **17**, 57–61.
23 Uhlmann H, Kraft R and Bernhardt R (1994) C-terminal region of adrenodoxin affects its structural integrity and determines differences in its electron transfer function to cytochrome P-450. *J Biol Chem* **269**, 22557–22564.
24 Sagara Y, Wada A, Takata Y, Waterman MR, Sekimizu K and Horiuchi T (1993) Direct expression of adrenodoxin reductase in *Escherichia coli* and the functional characterization. *Biol Pharm Bull* **16**, 627–630.
25 Omura T and Sato R (1964) The carbon monoxide-binding pigment of liver microsomes. i. evidence for its hemoprotein nature. *J Biol Chem* **239**, 2370–2378.
26 Litzenburger M, Kern F, Khatri Y and Bernhardt R (2015) Conversions of tricyclic antidepressants and antipsychotics with selected P450s from *Sorangium cellulosum* So ce56. *Drug Metab Dispos* **43**, 392–399.
27 Litzenburger M and Bernhardt R (2016) Selective oxidation of carotenoid-derived aroma compounds by CYP260B1 and CYP267B1 from *Sorangium cellulosum* So ce56. *Appl Microbiol Biotechnol* **100**, 4447–4457.
28 Denisov IG, Makris TM, Sligar SG and Schlichting I (2005) Structure and chemistry of cytochrome P450. *Chem Rev* **105**, 2253–2277.
29 Martinis SA, Atkins WM, Stayton PS and Sligar SG (1989) A conserved residue of cytochrome P-450 is involved in heme-oxygen stability and activation. *J Am Chem Soc* **111**, 9252–9253.
30 Zakzeski J, Jongerius AL and Weckhuysen BM (2010) Transition metal catalyzed oxidation of Alcell lignin, soda lignin, and lignin model compounds in ionic liquids. *Green Chem* **12**, 1225–1236.
31 Teutsch HG, Hasenfratz MP, Lesot A, Stoltz C, Garnier JM, Jeltsch JM, Durst F and Werck-Reichhart D (1993) Isolation and sequence of a cDNA encoding the Jerusalem artichoke cinnamate 4-hydroxylase, a major plant cytochrome P450 involved in the general phenylpropanoid pathway. *Proc Natl Acad Sci U S A* **90**, 4102–4106.
32 Vogt T (2010) Phenylpropanoid biosynthesis. *Mol Plant* **3**, 2–20.
33 Camm EL and Towers GHN (1973) Phenylalanine ammonia lyase. *Phytochemistry* **12**, 961–973.
34 Fahlbusch K-G, Hammerschmidt F-J, Panten J, Pickenhagen W, Schatkowski D, Bauer K, Garbe D and Surburg H (2000) *Flavors and Fragrances*. Wiley-VCH Verlag GmbH & Co. KGaA, Weinheim.
35 Khatri Y, Hannemann F, Ewen KM, Pistorius D, Perlova O, Kagawa N, Brachmann AO, Muller R and Bernhardt R (2010) The CYPome of *Sorangium cellulosum* So ce56 and identification of CYP109D1 as a new fatty acid hydroxylase. *Chem Biol* **17**, 1295–1305.
36 Meunier B, de Visser SP and Shaik S (2004) Mechanism of oxidation reactions catalyzed by cytochrome p450 enzymes. *Chem Rev* **104**, 3947–3980.
37 Watanabe K, Narimatsu S, Yamamoto I and Yoshimura H (1991) Oxygenation mechanism in conversion of aldehyde to carboxylic acid catalyzed by a cytochrome P-450 isozyme. *J Biol Chem* **266**, 2709–2711.
38 Raner GM, Hatchell JA, Dixon MU, Joy TL, Haddy AE and Johnston ER (2002) Regioselective peroxo-dependent heme alkylation in P450(BM3)-F87G by aromatic aldehydes: effects of alkylation on cataysis. *Biochemistry* **41**, 9601–9610.

Supporting information

Additional Supporting Information may be found online in the supporting information tab for this article:

Table S1. Forward and reversed primers used for the mutagenesis of CYP260B1

Table S2. Soret-peaks of CYP260B1 variants in oxidized, reduced, CO-bound, cinnamaldehyde-bound, and progesterone-bound state, respectively

Fig. S1. SDS/PAGE of the purification of CYP260B1 as well as purified single mutants (T224A and T232A) and double mutant (T224A/T232A)

Fig. S2. UV-Vis characterization of wild-type CYP260B1 (A), T224A (B), T232A (C), and T224A/T232A double mutant (D)

Fig. S3. Chromatograms of the conversion of progesterone by wild-type CYP260B1 (A), T224A mutant (B), T232A mutant (C), and T224A/T232A double mutant (D), respectively

Fig. S4. A, B, and C show the effect of radical scavengers on the catalytic rate of T224A, T232A, and T224A/T232A, respectively.